(16) ^{13}C NMR in C_6D_6: δ 324 (s, CCMe$_3$), 88.2 (t, J_{CH} = 111 Hz, CH$_2$CMe$_3$), 53.8 (s, CCMe$_3$), 34.1 (q, J_{CH} = 125 Hz, CMe$_3$), 33.6 (s, CH$_2$CMe$_3$), 30.3 (q, J_{CH} = 125 Hz, CMe$_3$).

(17) ^{13}C NMR in C_6D_6: δ 316 (J_{CP} = 14, J_{CW} = 210 Hz, CCMe$_3$), 286 (J_{CH} = 90, J_{CP} = 14, J_{CW} = 120 Hz, CHCMe$_3$), 53.5 (J_{CH} = 113, J_{CP} = 7, J_{CW} = 80 Hz, CH$_2$CMe$_3$), 52.4 (CMe$_3$), 47.0 (CMe$_3$), 38.3 (J_{CH} = 120 Hz, CMe$_3$), 34.3 (CMe$_3$), 33.4 (J_{CH} = 125, J_{CP} = 3 Hz, CMe$_3$), 32.6 (J_{CH} = 125, J_{CP} = 3 Hz. CMe$_3$), 22.0 (J_{CH} = 126, J_{CP} = 15 Hz, PMe$_3$).

(18) ^{1}H NMR in C_6D_6 at 270 MHz: τ 1.85 (t, 1, J_{HP} = 2.9 Hz, CHCMe$_3$), 8.62 (t, 18, J_{HP} = 3.3 Hz, PMe$_3$), 8.74 (s, 9, CMe$_3$), 8.75 (s, 9, CMe$_3$), 8.76 (s, 9, CMe$_3$), 8.78 (t, 2, J_{HP} = 18 Hz, CH$_2$CMe$_3$). On decoupling ^{31}P, all triplets sharpen to singlets.

(19) R. R. Schrock and J. D. Fellmann, *J. Am. Chem. Soc.*, **100**, 3359 (1978).

(20) The m/e 546 parent ion is not seen. A typical pattern starting at m/e 477 corresponds to loss of a neopentyl group. It overlaps with a pattern about one fifth as intense starting at m/e 478 which *formally* corresponds to loss of a neopentylidene fragment from m/e 548.

(21) M. R. Churchill and W. J. Youngs, private communication.

(22) Calcd: 544. Found in cyclohexane: 531 (concentration, 0.033 M).

(23) ^{13}C{^{1}H} NMR in C_6D_6: δ 296 (t, $J_{CP} \approx J_{CP'} \approx$ 12 Hz, CCMe$_3$), 256 (dd, J_{CP} = 13, $J_{CP'}$ = 31 Hz, CHCMe$_3$; J_{CH} = 84 Hz in the gated spectrum), 54.7 (t, $J_{CP} \approx J_{CP'}$ = 4 Hz, CH$_2$CMe$_3$), 51.7 (s, CMe$_3$), 47.7 (s, CMe$_3$), 34.0 (s, CMe$_3$), 36.4 (s, CMe$_3$), 34.6 (s, CMe$_3$), 33.0 (t, $J_{CP} \approx J_{CP'}$ = 3, CMe$_3$). The dmpe carbon atoms give rise to a complex non-first-order pattern from 32 to 12 ppm.

(24) Two likely possibilities are a neopentylidene or a neopentylidyne hydride complex (no ν_{MH} is obvious in the IR spectrum). An extremely broad low-field resonance can be seen after exhaustive pulsing. All P nuclei may be different and/or the molecule may be fluxional. Variable-temperature and ^{31}P decoupling experiments are in progress.

(25) Alfred P. Sloan Foundation Fellow, 1976–1978.

D. N. Clark, R. R. Schrock*[25]

Department of Chemistry
Massachusetts Institute of Technology
Cambridge, Massachusetts 02139

Figure 1. UV–visible spectra of Ag$_{1,2,3}$/Ar mixtures (Ag/Ar $\simeq$ 1/10^3) at 12 K. Note the growth of Ag$_2$ and Ag$_3$ clusters and loss of Ag atoms as a result of 305-nm Ag atom excitation. Spectra A, B, and C represent irradiation times of 0, 1. and 4 min, respectively.

Relative Extinction Coefficient Measurements for Naked Silver Atom Clusters, Ag$_{1,2,3}$, by Photoaggregation Techniques

Sir:

Ligand-free molecular clusters containing only several transition metal atoms are currently becoming accessible for detailed spectroscopic and chemical studies.[1] Naked molecular clusters are of considerable interest in a wide area which includes both homogeneous and heterogeneous catalysis. In particular, one may think in terms of modeling the active centers of highly dispersed heterogeneous catalysts, using very small metal atom clusters of variable but precisely defined size. Another attractive proposition is that the electronic structure of metal atom cluster complexes, which are often active homogeneous catalysts, may be elucidated through combined experimental and theoretical studies of the corresponding metal atom framework.

We have reported a cryochemical preparative route to transition metal atom clusters, involving photoinduced diffusion and aggregation of matrix-isolated metal atoms, monitored by ultraviolet–visible absorption spectroscopy.[2] In this communication we report an application of this technique to the measurement of molar extinction coefficients, relative to atomic species, for diatomic and triatomic silver.

Extinction coefficient information is of fundamental importance in quantitative studies of the chemistry and photochemistry of transition metal atom clusters, and in the analysis of metal atom recombination kinetics. Relative extinction coefficients for transition metal diatomic molecules, $\epsilon_{M_2}/\epsilon_M$, as determined by quantitative metal atom deposition studies, have been reported.[3] However, we would suggest that the controlled photoaggregation technique allows for a more convenient and accurate evaluation of these quantities. Moreover, an extension of this technique to higher clusters is also possible.
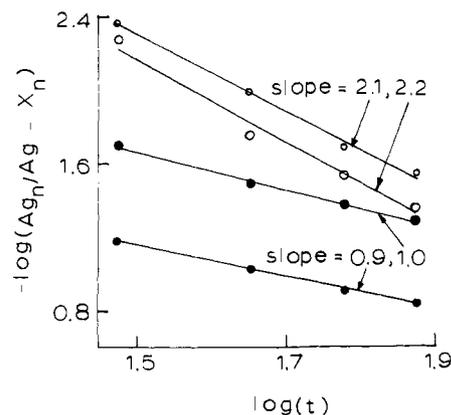
Figure 2. Kinetic plots showing a linear dependence on irradiation time (305 nm) of the absorbance ratios Ag$_2^{263nm}$/Ag^{300nm} and Ag$_2^{390nm}$/Ag^{300nm} (O) and a linear dependence on the square of irradiation time of the absorbance ratios Ag$_3^{245nm}$/Ag^{300nm} and Ag$_3^{440nm}$/Ag^{300nm} (●), as predicted from the simple kinetic analysis. The quantities X_n were chosen in order to shift the Ag$_2$/Ag vs. t and Ag$_3$/Ag vs. t^2 plots through the origin. Details will be described in the full paper.

The cryophotoclustering technique is illustrated for Ag atoms in Figure 1. Kinetic studies of the clustering process are now in progress and the results will be described in detail in a forthcoming publication. Preliminary results have indicated that, under certain conditions, the rates of formation of diatomic and triatomic silver may usefully be approximated by simple second-order kinetics. A simple analysis predicts that the slope of a log (Ag$_n$/Ag) vs. log (t) plot, where Ag$_n$ and Ag represent absorbances and t represents the irradiation time, should have a value of 1.0 for n = 2 and 2.0 for n = 3. These plots are shown in Figure 2. The observed slopes, 0.9/1.0 and 2.1/2.2 support our Ag$_2$ and Ag$_3$ assignments, which are indicated in Figure 1. These assignments correlate exactly with earlier assignments based on Ag atom concentration experiments.[2a]

Simple mass–balance considerations lead to the following expression which relates the decrease in an atomic absorption

Table I. Relative Extinction Coefficients[a] for Ag_2 and Ag_3

	peak height	peak area
$\epsilon_1^{315}/\epsilon_2^{260}$ (Ar)	0.8 ± 0.2	0.40 ± 0.05
$\epsilon_1^{315}/\epsilon_3^{245}$ (Ar)	1.2 ± 0.5	0.6 ± 0.3
$\epsilon_1^{323}/\epsilon_2^{270}$ (Kr)		0.43 ± 0.05

[a] The corresponding wavelengths (nm) in Ar and Kr matrices are indicated as superscripts. The uncertainty limits represent estimated upper and lower bounds.

to increases in diatomic and triatomic absorptions in terms of the appropriate extinction coefficients:

$$(A_1' - A_1'') = 2\epsilon_1/\epsilon_2(A_2'' - A_2') + 3\epsilon_1/\epsilon_3(A_3'' - A_3') \quad (1)$$

It is prearranged in these experiments that Ag_4 and higher clusters are not produced in significant quantities. A_n' represents the absorbance due to Ag_n at time t', A_n'' is the absorbance due to Ag_n at time t'', and ϵ_n represents the molar extinction coefficients for Ag_n.

For very dilute conditions and short irradiation times, we can arrange that only negligible quantities of Ag_3 are formed so that eq 1 may be solved directly for ϵ_1/ϵ_2. For longer irradiation times the complete eq 1 may be used to obtain a value for ϵ_1/ϵ_3. We note here that a similar procedure, using multiple depositions at different concentrations, may also be used. However, the advantage of the photoaggregation method is that only one deposition is required for each ϵ_1/ϵ_2 or ϵ_1/ϵ_3 determination, so that the method is much more convenient and considerably more accurate since mass balance of total metal is maintained after each irradiation, thus eliminating the need for multiple quantitative depositions.

The extinction coefficient results are summarized in Table I where ϵ_1/ϵ_2 and ϵ_1/ϵ_3 values for Ag/Ar matrices are given for both peak-height and peak-area measurements. The value of ϵ_1/ϵ_2 was determined by both the photoaggregation and deposition procedures and the results were in satisfactory agreement. The results in Table I show that ϵ_1/ϵ_2 is essentially invariant, within experimental error, to the change from Ar to Kr matrices. It is appropriate to note here that the final cluster size distribution is quite different in Ar compared with Kr matrices. Thus, in Ar matrices Ag_3 forms readily on irradiation, but only to a very small extent in Kr matrices. The possibility of exploiting this matrix dependence to produce very narrow cluster size distributions will be discussed elsewhere.

References and Notes

(1) (a) G. A. Ozin. *Catal. Rev.—Sci. Eng.*, **16**, 191 (1977), and references cited therein; (b) H. Huber and G. A. Ozin, "Selective Naked Cluster Cryophotochemistry: Trisilver", paper presented at the 175th National Meeting of the American Chemical Society, Anaheim, Calif., March 13–17, 1978, and *Inorg. Chem.*, in press; (c) A. J. Lee Hanlan and G. A. Ozin, *ibid.*, **16**, 2857 (1977); (d) M. Moskovits and J. E. Hulse. *J. Chem. Phys.*, **67**, 4271 (1977).
(2) (a) G. A. Ozin and H. Huber, *Inorg. Chem.*, **17**, 155 (1978); (b) G. A. Ozin and W. E. Klotzbücher, *J. Mol. Catal.*, **3**, 195 (1977/78), and *J. Am. Chem. Soc.*, **100**, 2262 (1978); (c) S. A. Mitchell and G. A. Ozin, in preparation.
(3) M. Moskovits and G. A. Ozin in "Cryochemistry", M. Moskovits and G. A. Ozin, Ed., Wiley, New York, 1976, and references therein.

Steven A. Mitchell, Geoffrey A. Ozin*

Lash Miller Chemical Laboratories and Erindale College University of Toronto, Toronto, Ontario, Canada M5S 1A1
Received April 6, 1978

Structural Identification of the Extruded Cores of the Active Centers of Iron–Sulfur Proteins by Fluorine-19 Nuclear Magnetic Resonance Spectroscopy. Application to Milk Xanthine Oxidase

Sir:

The core extrusion method for identification of active centers in iron–sulfur proteins, as developed in this[1–4] and another laboratory,[5–7] is based on the ligand exchange reaction (eq 1)

holoprotein + RSH

$$\rightarrow \begin{Bmatrix} [Fe_2S_2(SR)_4]^{2-} \\ \text{and/or} \\ [Fe_4S_4(SR)_4]^{2-} \end{Bmatrix} + \text{apoprotein} \quad (1)$$
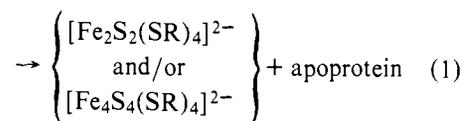
conducted with excess thiol in a medium capable of unfolding protein tertiary structure. In usual practice the reaction solution after extrusion is complete is examined spectrophotometrically at 400–700 nm in order to determine the type and number (n_d, Fe_2S_2; n_t, Fe_4S_4) of Fe–S centers removed from a protein molecule. Spectrophotometric assay of extrusion products is unsatisfactory for proteins containing visible chromophores (e.g., flavin) or components (e.g., Mo) possibly capable of forming such chromophores upon reaction with thiol, unless suitable blanks are available[3] or recourse is taken to separation procedures. To circumvent this difficulty[7b] we have developed a ^{19}F FT NMR method of identification of extruded protein core structure which is based on the paramagnetism of $[Fe_2S_2(SR)_4]^{2-}$ and $[Fe_4S_4(SR)_4]^{2-}$ complexes and the attendant sensitivity of their contact-shifted resonances[8–10] to differences in these structures.

p-Trifluoromethylbenzenethiol[11] (δ 9.5), $(Et_4N)_2$-$[Fe_2S_2(SR_F)_4]$[12,13] (δ 3.7, ϵ_M^{476} 11 200), and $(Et_4N)_2$-$[Fe_4S_4(SR_F)_4]$[14] (δ 6.4, ϵ_M^{452} 18 000) were prepared by published procedures; band maxima (nanometers), extinction coefficients, and ^{19}F chemical shifts (parts per million at -15 °C relative to $PhCFCl_2$) as determined in the extrusion medium (4:1 v/v $HMPA/H_2O$ (50 mM TrisCl, pH 8.5), R_FSH/Fe mol ratio $\sim$100/1) used throughout this work are indicated. The efficacy of R_FSH as an extrusion reagent was first investigated using the spectrophotometric method[2] as applied to *Clostridium pasteurianum* Fd_{ox}[15] (A_{390}/A_{285} 0.80, mol wt 6200, 2 Fe_4S_4) and spinach Fd_{ox}[16] (A_{420}/A_{285} 0.44, mol wt 10 660, 1 Fe_2S_2) preparations.[17] The following data reveal R_FSH to be as effective as $PhSH$[1,2] under comparable conditions: *C. pasteurianum* Fd_{ox}, seven determinations (9–25 μM), R_FSH/Fe 55–150/1, $\bar{n}_t = 1.94 \pm 0.02$; spinach Fd_{ox}, six determinations (25–44 μM), R_FSH/Fe 100–400/1, $\bar{n}_d = 1.00 \pm 0.09$.

The ^{19}F FT NMR method of extruded protein core structure identification is illustrated with *C. pasteurianum* Fd_{ox} and spinach Fd_{ox} in Figure 1, where experimental conditions are defined. As in the spectrophotometric procedure, aqueous protein buffer solutions are diluted 5-fold with HMPA containing R_FSH, the extrusion reaction is allowed to proceed to completion at 25 °C, and the ^{19}F spectrum is then acquired at -15 °C, at which temperature the limit of slow exchange between free R_FSH and coordinated thiolate is attained or very closely approached. Chemical shifts and line widths are the same as those of $[Fe_2S_2(SR_F)_4]^{2-}$ and $[Fe_4S_4(SR_F)_4]^{2-}$ measured separately under the same conditions. Complete signal resolution of these complexes and of the large excess of R_FSH is apparent; contact shifts of -5.8 ($[Fe_2S_2(SR_F)_4]^{2-}$ and -3.1 ppm ($[Fe_4S_4(SR_F)_4]^{2-}$) are obtained from the chemical shifts. Note that the presence of 4 CF_3 groups affords a factor of 12 in equivalent ^{19}F concentration over M (complex). Quantitation is achieved by addition of a fixed amount